INSTITUTE OF PHYSICS PUBLISHING JOURNAL OF OPTICS A: PURE AND APPLIED OPTICS

J. Opt. A: Pure Appl. Opt. **8** (2006) 831–834 doi:10.1088/1464-4258/8/10/002

Subwavelength imaging by a dielectric-tube photonic crystal

Zhixiang Tang[1,2], Hao Zhang[3], Runwu Peng[1,2], Yunxia Ye[1], Chujun Zhao[1], Shuangchun Wen[2] and Dianyuan Fan[1]

[1] Shanghai Institute of Optics and Fine Mechanics, Chinese Academy of Sciences, PO Box 800-211, Shanghai 201800, People's Republic of China
[2] School of Computer and Communication, Hunan University, Changsha 410082, People's Republic of China
[3] Department of Optical Science and Engineering, Fudan University, Shanghai 200433, People's Republic of China

Received 7 May 2006, accepted for publication 10 July 2006
Published 7 August 2006
Online at stacks.iop.org/JOptA/8/831

Abstract
In contrast to previous two-dimensional coated photonic crystals, in this paper we propose a left-handed one that is made of dielectric tubes arranged in a close-packed hexagonal lattice. Without metallic cores, this structure is low-loss and convenient to fabricate. Negative refraction and its resulting focusing are investigated by dispersion characteristic analysis and numerical simulation of the field pattern. With proper modification at the interface, the image is improved. With better isotropy than that with noncircular rods, planoconcave lenses made by dielectric tubes focus a Gaussian beam exactly at $R/|n-1|$.

Keywords: left-handed materials, photonic crystal, superlens

(Some figures in this article are in colour only in the electronic version)

1. Introduction

Negative refraction is an unusual optical phenomenon in which electromagnetic waves refract in the opposite directions to what are normally observed in conventional dielectric materials [1–5]. This peculiar phenomenon was first predicted in left-handed material (LHM), which is characterized by simultaneous negative permittivity and permeability [1]. An important application of negative refraction materials is the flat lens [6–8]. More interestingly, a flat lens with an effective refraction index of $n_{\text{eff}} = -1$ can overcome the diffraction limit [8]. During the past few years, negative refraction and its resulting focusing have attracted a great deal of attention and considerable progress has been made in fabricating such a metamaterial [4, 5, 9, 10].

In general, there are two underlying mechanisms for negative refraction [11–14]. One is left-handed behaviour as being theoretically studied by Veselago [1]. In this case, because of simultaneous negative permittivity and permeability, the electromagnetic fields $\boldsymbol{E}$, $\boldsymbol{H}$ and the wavevector $\boldsymbol{k}$ form a left-handed triplet (i.e., $\boldsymbol{S}\cdot\boldsymbol{k} < 0$, where $\boldsymbol{S}$ is the Poynting vector). Due to anisotropy (i.e., $\boldsymbol{S}\cdot\boldsymbol{k} > 0$, but $\boldsymbol{S}$ and $\boldsymbol{k}$ are noncollinear), other negative refraction may occur under certain conditions [13, 14]. Both of these two negative refractions have been demonstrated in two-dimensional (2D) photonic crystals (PhCs) theoretically and experimentally [5–7, 11–15].

Recently, Zhang has intensively studied negative refraction and its resulting subwavelength imaging in 2D coated PhCs, which were fabricated by adding a fraction of a metallic component to the centre of each dielectric cylinder [16–19]. Because of the metallic cores, this PhC is lossy and inconvenient to fabricate. For the purpose of improvement, in this paper we propose an 2D PhC that is made of dielectric tubes arranged in a close-packed hexagonal lattice [20]. Subwavelength imaging by this PhC is investigated through dispersion characteristic analysis and numerical simulation of the field pattern.

The rest of this paper is organized as follows. In section 2, we theoretically analyse the dispersion characteristics by examining the photonic band structure and equifrequency contours (EFCs). The numerical simulations of the field patterns are shown in section 3. Finally, we conclude this paper in section 4.

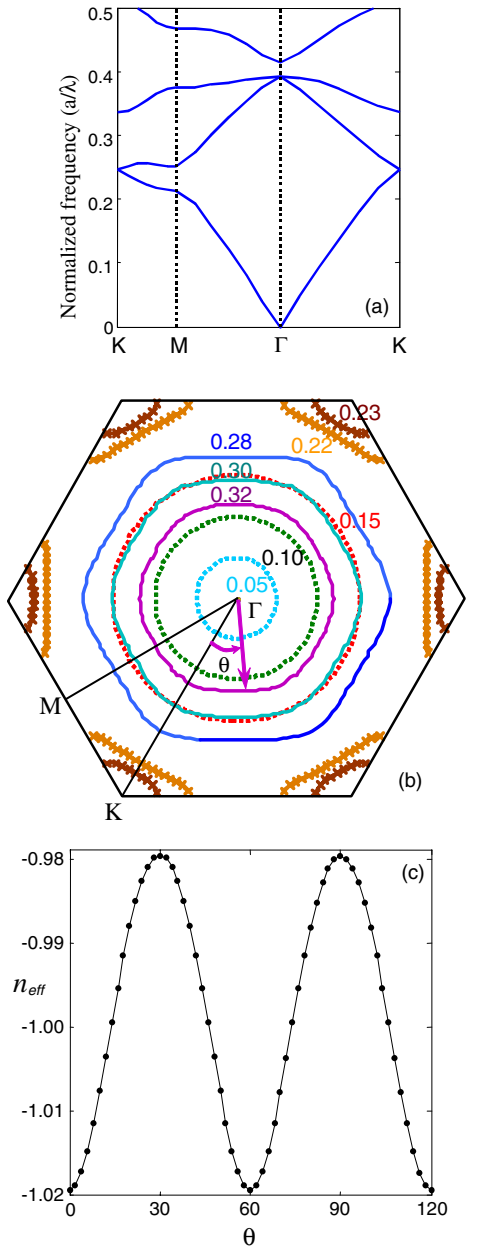

Figure 1. Dispersion characteristic analysis of the TM polarization for the 2D dielectric-tube PhC. (a) Photonic band structure. (b) Several EFCs of the lowest two bands. (c) Angle-dependent effective index $n_{\text{eff}}(\theta)$ at the normalized frequency $\omega_0 = 0.32$.

2. Dispersion characteristic analysis

In contrast to Zhang's coated PhC, the 2D PhC considered in this paper is made of dielectric tubes arranged in a close-packed hexagonal lattice. The dielectric constant of these tubes is $\varepsilon = 12.96$ (e.g., GaAs or Si at 1.55 μm). The absorption of the dielectric is neglected. The inside and outside diameters of each tube are $0.38a$ and $0.50a$ respectively, where a is the lattice constant. Without the metallic components, our PhC is low-loss. In addition, this structure can be fabricated as a PhC fibre. For this PhC, we only consider TM polarization; i.e., that the electric field E_z is parallel to these tubes.

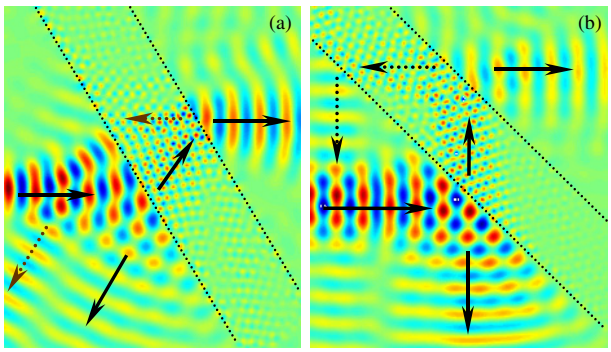

Figure 2. Negative refractions for two incident angles: (a) $\alpha = 30°$ and (b) $\alpha = 45°$.

The photonic band structure and several EFCs of this PhC are calculated by the plane wave expansion method and plotted in figure 1. The frequency is normalized as a/λ. From figures 1(a) and (b), we can see clearly that the PhC behaves in a left-handed manner in the second band [9]. For strongly modulated PhCs, the effective index can be written as

$$n_{\text{eff}} = \boldsymbol{k}/\boldsymbol{k}_0 = \text{sgn}(\boldsymbol{k} \cdot \boldsymbol{v}_{\text{g}})|\boldsymbol{k}|/|\boldsymbol{k}_0|, \tag{1}$$

where $\boldsymbol{k}$ and $\boldsymbol{k}_0$ are the wavevectors of light in PhC and free space, respectively, and sgn is the sign function. $\boldsymbol{v}_{\text{g}}$ is the group velocity in the PhC, which is given by

$$\boldsymbol{v}_{\text{g}} = \nabla_{\boldsymbol{k}}\omega(\boldsymbol{k}). \tag{2}$$

For the dielectric tube PhC we considered, the effective index $n_{\text{eff}} = -1$ is found at the normalized frequency $\omega_0 = 0.32$ whose EFC is nearly a circle, as shown in figure 1(b). The angle-dependent effective index $n_{\text{eff}}(\omega_0, \theta)$ is plotted in figure 1(c). Because of the near isotropy, $n_{\text{eff}}(\omega_0, \theta)$ varies between -1.02 and -0.98 with the angle θ.

3. Numerical simulations

To test the above analysis, numerical simulations are performed using the finite difference time domain (FDTD) method [21] with a treatment of perfectly matched layers [22]. Considering the inactive modes along the direction ΓM, which result from the symmetry of the eigenmodes of this PhC, the interface between the PhC and free space is arranged along ΓK [23].

We first consider a Gaussian beam with a normalized frequency $\omega_0 = 0.32$ incident to the PhC with angles $\alpha = 30°$ and $\alpha = 45°$. The propagation maps are illustrated in figures 2(a) and (b), respectively. For these two circumstances, it is clear that these incident beams refract in the opposite directions of their corresponding reflected beams, indicating that the effective index of the PhC is $n_{\text{eff}} = -1$.

Negative refraction allows a flat slab to behave as a lens. More importantly, a flat lens with $n_{\text{eff}} = -1$ can overcome the diffraction limit. In the following, we demonstrate subwavelength imaging by this flat PhC slab. A 7×30 PhC slab is taken as an example. To excite the surface waves efficiently, as sketched in figures 3 and 4, the PhC slabs are cut away $0.2a$ at each interface [12, 24]. First, we locate a continuous-wave point source with normalized frequency $\omega_0 = 0.32$ at

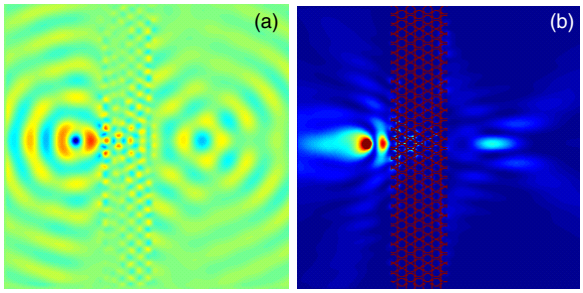

Figure 3. Propagation maps for the surface-modified flat superlens. The distance from the source to the first row of the PhC is $d_o = 2.6a$. (a) Snapshots of the electric field. (b) Average intensity over a period.

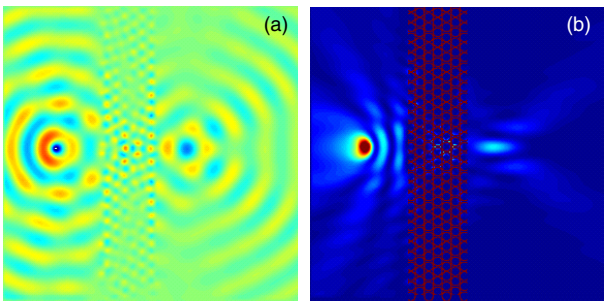

Figure 4. The same as figure 3, except $d_o = 4.6a$.

$d_o = 2.6a$ before the centre of the first row. As shown in figure 3, an image is formed at $d_i = 4.8a$ away from the centre of the last row. Compared with the PhC slab without cut, the image is moved $0.6a$ closer to the source (i.e., for the slab without cut, $d_i' = 5.4a$) and its full width at the half maximum (FWHM) decreases from 0.544λ (without cut) to 0.384λ, as plotted in figure 5. The improvement of the image can be interpreted with the distance between the source and the image $d_{oi} = d_o + d_{slab} + d_i$, where d_{slab} is the centre distance between the first and the last rows. The distance is $d_{oi}' = 4.22\lambda$ for the PhC slab without cut and $d_{oi} = 4.03\lambda$ for the PhC slab with $0.2a$ cut. Owe to resonant excitations of the surface waves at the interface, the subwavelength image is improved [12, 24]. To see the dependence of the image on the object distance, we move the source to $d_o = 4.6a$. In figure 4, the image is moved to $d_i = 2.85a$. It is obvious that the distance between the source and the image is a constant ($d_{oi} = \text{const}$), which is required by Snell's law for a flat lens with $n_{eff} = -1$.

Another novel application of negative refraction is the planoconcave lens [25, 26]. A planoconcave lens made by this PhC is shown in figure 6. First, we consider a Gaussian beam with normalized frequency $\omega_0 = 0.32$ incident to the planoconcave lens perpendicularly. In contrast to a planoconcave lens made by an elliptical-rod PhC [12], a focus is formed truly at the midpoint of the radius (i.e. $R/|n-1|$), as illustrated in figure 6(a). The FWHM of the focus is 0.576λ. Similarly to [12, 25], this photograph is composed of two surface plots. On the left-hand side of the white strip, the field map of the incident beam is shown, and on the right-hand side is the average intensity over a period. In figure 6(b), a continuous-wave point source is located at the focus, and a quasi-plane wave is formed out of the planoconcave lens.

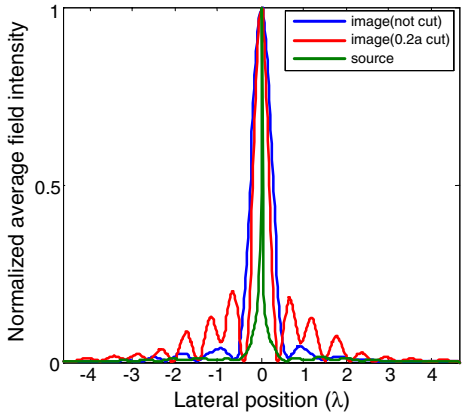

Figure 5. The transverse normalized intensity of the source and the images. The FWHM of the image is improved from 0.554λ to 0.384λ for a $0.2a$ cut.

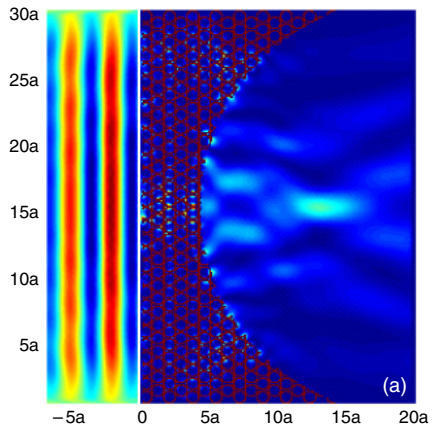

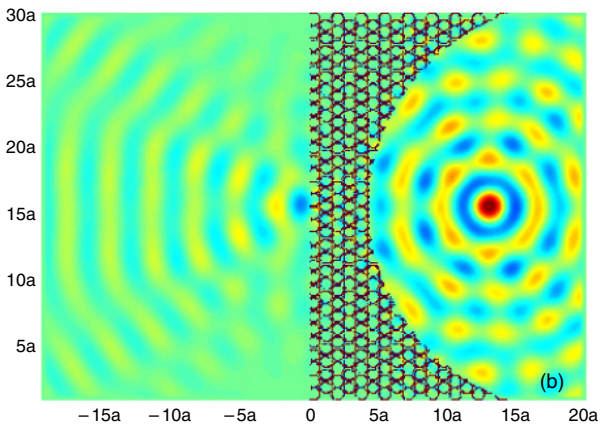

Figure 6. (a) Focusing by planoconcave lens. (b) Field maps of the incident point source and the emerging quasi-plane wave.

4. Conclusions

In summary, we have systematically investigated a 2D PhC that is made of dielectric tubes arranged in a close-packed

hexagonal lattice. Compared with Zhang's coated PhC, our PhC is low-loss and convenient to fabricate. Negative refraction and its resulting focusing by this PhC have been investigated through dispersion characteristic analysis and numerical simulation of the field pattern. With proper modification at the PhC surface, the subwavelength images have been improved. Because of the near isotropy, the focus of the PhC planoconcave lens locates exactly at the midpoint of the radius, i.e., $R/|n-1|$. Experiments are expected to demonstrate our theoretical results.

Acknowledgments

This work is partially supported by the Natural Science Foundation of China (Grant Nos. 10576012 and 60538010), the National High Technology Research and Development Program of China (Grant No. 2004AA84ts12).

References

[1] Veselago V G 1968 *Sov. Phys.—Usp.* **10** 509–14
[2] Kosaka H, Kawashima T, Tomita A, Notomi M, Tamamura T, Sato T and Kawakami S 1998 *Phys. Rev.* B **58** R10096–9
[3] Zhang Y, Fluegel B and Mascarenhas A 2003 *Phys. Rev. Lett.* **91** 157404
[4] Shelby R A, Smith D R and Schultz S 2001 *Science* **292** 77–9
[5] Cubukcu E, Aydin K, Ozbay E, Foteinopoulou S and Soukoulis C M 2003 *Nature* **423** 604–5
[6] Parimi P V, Lu W T, Vodo P and Sridhar S 2003 *Nature* **426** 404
[7] Moussa R, Foteinopoulou S, Zhang L, Tuttle G, Guven K, Ozbay E and Soukoulis C M 2005 *Phys. Rev.* B **71** 085106
[8] Pendry J B 2000 *Phys. Rev. Lett.* **85** 3966–9
[9] Notomi M 2000 *Phys. Rev.* B **62** 10696–705
[10] Chen H, Ran L, Jiantao, Huangfu, Zhang X, Chen K, Grzegorczyk T M and Kong J A 2004 *Phys. Rev.* E **70** 057605
[11] Martinez A and Marti J 2005 *Opt. Express* **13** 2858–68
[12] Tang Z, Peng R, Fan D, Wen S, Zhang H and Qian L 2005 *Opt. Express* **13** 9796–803
[13] Luo C, Johnson S G, Joannopoulos J D and Pendry J B 2002 *Phys. Rev.* B **65** R201104
[14] Foteinopoulou S and Soukoulis C M 2003 *Phys. Rev.* B **67** 235107
[15] Gajić R, Meisels R, Kuchar F and Hingerl K 2005 *Opt. Express* **13** 8596–605
[16] Zhang X 2004 *Phys. Rev.* B **70** 195110
[17] Zhang X 2005 *Phys. Rev.* E **71** 037601
[18] Zhang X and Li L-M 2005 *Appl. Phys. Lett.* **86** 121103
[19] Zhang X 2005 *Phys. Rev.* B **70** 205102
[20] Kurt H and Citrin D S 2005 *Opt. Express* **13** 10316–26
[21] Taflove A and Hagness S C 2000 *Computational Electrodynamics: The Finite-Difference Time-Domain Method* 2nd edn (Boston, MA: Artech House Publishers)
[22] Berenger J P 1991 *J. Comput. Phys.* **114** 185–200
[23] Sakoda K 2001 *Optical Properties of Photonic Crystals* (Berlin: Springer)
[24] Xiao S, Qiu M, Ruan Z and He S 2004 *Appl. Phys. Lett.* **85** 4269–71
[25] Vodo P, Parimi P V, Lu W T and Sridhar S 2005 *Appl. Phys. Lett.* **86** 201108
[26] Parazzoli C G, Greegor R B, Nielsen J A, Thompson M A, Li K, Vetter A M, Tanielian M H and Vier D C 2004 *Appl. Phys. Lett.* **84** 3232–4